



The impact of global warming and the El Niño–Southern Oscillation on seasonal precipitation extremes in Australia

François P. D. Delage¹ · Scott B. Power¹

Received: 11 July 2019 / Accepted: 7 April 2020 / Published online: 28 April 2020
© The Author(s) 2020

Abstract

The El Niño–Southern Oscillation (ENSO) drives substantial variability in precipitation and drought risk over Australia. Understanding the combined effect of anthropogenic forcing and ENSO on Australian precipitation extremes over the coming century can assist adaptation efforts. Here we use 24 CMIP5 climate models to examine externally forced changes in the frequency of “droughts”, when precipitation falls below the pre-industrial Decile 1 threshold. We focus on June to November (i.e., southern hemisphere Winter–Spring season) because precipitation during this period is important for agricultural production and recharging reservoirs in many parts of the country. The analysis in this paper is based on two 90-year simulations (1900–1989 and 2010–2099) for Historical and RCP8.5 scenarios. We show that the frequency of droughts, including droughts occurring in consecutive Winter–Spring seasons, is projected to increase in the twenty-first century under the RCP8.5 scenario in all eight Natural Resource Management (NRM) “clusters”. Approximately 60% of years are projected to be drought years in Perth, 35% in Adelaide, 30% in Melbourne, and approximately 20–25% of years in Sydney, Canberra and Brisbane. The relative frequency distributions of seasonally averaged Winter–Spring precipitation shift to lower values in all NRM clusters. However, apart from the Southern and Southwestern Flatlands, the shifts are accompanied by changes in the shape of the distributions whereby the high end of the distributions do not shift as much as other parts of the distribution and the wettest seasons become marginally wetter. This means that in most locations generally drier conditions are projected to be infrequently punctuated by seasons that are just as wet or wetter than the wettest years experienced during the twentieth century. While the models generally do a poor job in simulating ENSO precipitation teleconnections over Australia, an increase in ENSO-driven variability is suggested for the Wet Tropics, the Monsoonal North, the Central Slopes and the Southern and Southwestern Flatlands.

1 Introduction

Precipitation in Australia is projected to change in response to further global warming and in some regions, appears to have already been affected (CSIRO and Bureau of Meteorology 2015). In southern Australia “cool season (Winter and Spring) rainfall is projected to decrease (high confidence), though little change or increases in Tasmania in winter are projected (medium confidence). The winter decline may be as great as 50% in south-western Australia in the highest emission scenario (RCP8.5) by 2090”, in eastern Australia “For late in the century (2090), there is medium confidence in a winter rainfall decrease”, and in northern Australia

“there is low confidence in the direction of future rainfall change for late in the century” (CSIRO and Bureau of Meteorology 2015).

More recently Power and Delage (2018) pointed out that the precipitation during future El Niño–Southern Oscillation (ENSO) years is a function of both mean-state changes and changes in ENSO-driven variability. They concluded, however, that while precipitation variability in CMIP5 models associated with ENSO is projected to increase in the tropical Pacific and corresponding increases are evident in many regions away from the Equatorial Pacific, the increases are modest, and are robust in only a handful of regions. They considered two large boxes involving Australia—one for “Northern Australia” and another for “Southern Australia/New Zealand” combined. They found no clear evidence of any change in ENSO-driven rainfall variability in either of these broad regions. They concluded, however, that “during the latter

✉ François P. D. Delage
Francois.Delage@bom.gov.au

¹ Bureau of Meteorology, Melbourne, VIC, Australia

half of the twenty-first century under the RCP8.5 scenario ENSO-driven precipitation variability ... will occur about average conditions that are very different to those experienced during the twentieth century”.

CSIRO and Bureau of Meteorology (2015) also provided projections for drought in Australia concluding that “the time in drought is projected to increase over southern Australia with high confidence, consistent with the projected decline in mean rainfall. Time in drought is projected to increase with medium or low confidence in other regions. The nature of droughts is also projected to change with a greater frequency of extreme droughts, and less frequent moderate to severe drought projected for all regions (medium confidence)”. These conclusions were based on the Standardised Precipitation Index (CSIRO and Bureau of Meteorology 2015).

CSIRO and Bureau of Meteorology (2015) also concluded that “extreme rainfall events (wettest day of the year and wettest day in 20 years) are projected to increase in intensity with high confidence. Confidence is reduced to medium confidence for south-western Western Australia, where the reduction in mean rainfall may be so strong as to significantly weaken this tendency”.

The purpose of this investigation is to examine important, related issues not examined previously or examine in greater depth key issues that have been investigated before:

- While previous studies have examined changes in dry and wet conditions in the twenty-first century relative to the historical period, here we examine changes relative to both pre-industrial and historical conditions. This allows us to estimate the total impact of external forcing, and the extent to which external forcing influenced historical climate.
- Unlike previous studies we examine changes in both Decile 1 and Decile 9 thresholds as well as changes in the magnitude of the highest and lowest seasonal values on record.
- We also examine the role that ENSO plays in driving extreme precipitation in the twenty-first century at a smaller spatial scale than has been done previously (Power and Delage 2018).
- We also examine—for the first time in an Australian context—the impact of global warming on the likelihood of experiencing drought in consecutive Winter–Spring seasons.

Particular attention is given to eight Natural Resource Management (NRM) clusters (CSIRO and Bureau of Meteorology 2015) depicted in Fig. 1. We focus on changes during Winter–Spring (i.e., June–November), when precipitation is important for growing crops and replenishing dams in many regions.

This paper is organised as follows. The data, models and methods used are described in Sect. 2. Results are presented in Sect. 3, and are summarised and discussed in Sect. 4. Caveats are provided in the same section.

2 Methods

2.1 Models and forcing scenarios

Twenty-four models (see Table 1) from the CMIP5 archive (Taylor et al. 2007) forced using pre-industrial control conditions, historical conditions over the period 1900–2005 and the RCP8.5 scenario over the period 2006–2100 are used. Details on the “business-as-usual” RCP8.5 scenario are provided elsewhere (Moss et al. 2010; van Vuuren et al. 2011). The analysis in this paper is based on 90-year simulations (1900–1989 and 2010–2099) and 450-year-long preindustrial simulations. Only models which have simulations for all these periods are included in the analysis. All coupled climate models and the observations were re-gridded to a 1.5° latitude/1.5° longitude grid prior to analysis. All results in this paper are based on June–November average precipitation.

2.2 Observations

For the observations we use the Australian Water Availability Project (AWAP) precipitation data set (Raupach et al. 2009) over 1900–2017 and HadSST3 sea-surface temperature data (Morice et al. 2012).

2.3 Classification of El Niño, neutral and La Niña years

The method used to define El Niño, neutral and La Niña years is based on detrended November–April SST anomalies in the NINO3.4 region (5° N–5° S, 170° W–120° W). Detrending was accomplished by removing the cubic spline from the NINO3.4 timeseries. The magnitude and sign of the resulting time-series in the observations and each model, $N3.4^*(t)$ say, was then used to classify years as El Niño, La Niña, or neutral years using $N3.4^* > 0.8\sigma$, $N3.4^* < -0.8\sigma$ or $-0.8\sigma \leq N3.4^* \leq +0.8\sigma$, respectively. Here σ is the standard deviation of $N3.4^*(t)$ in the observations and each model, and t is time.

2.4 NRM clusters

We consider eight NRM clusters (CSIRO and Bureau of Meteorology 2015) in some of the analysis: the Central Slopes (CS), the East Coast (EC), the Monsoonal North (MN), the Murray Basin (MB), the Rangelands (R), the

Fig. 1 The Natural Resource Management (NRM) regions used in some of the analysis. Source: CSIRO and Bureau of Meteorology (2015)

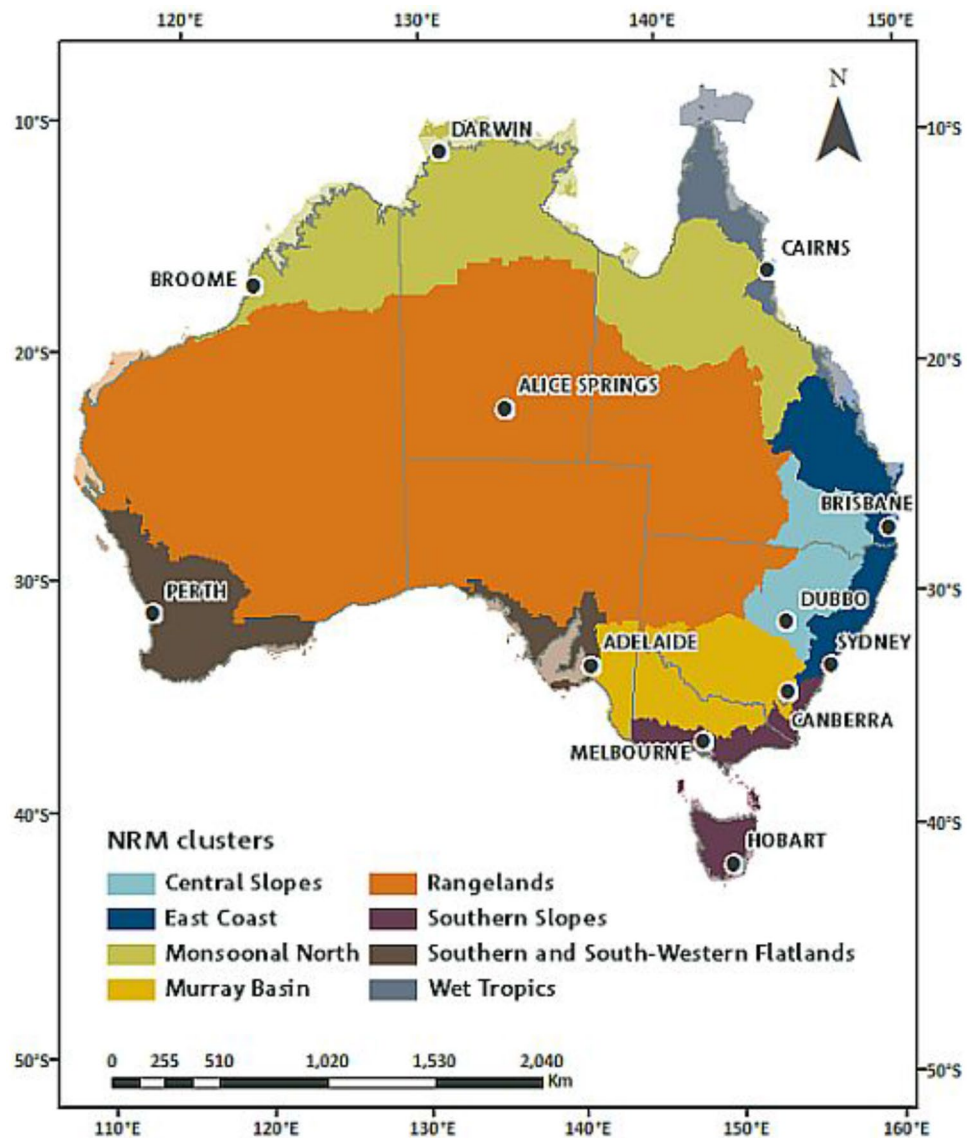


Table 1 The 24 models used

No.	Model name	No.	Model name
1	ACCESS1-0	13	GFDL-CM3
2	ACCESS1-3	14	GFDL-ESM2G
3	bcc-csm1-1	15	GFDL-ESM2M
4	BNU-ESM	16	HadGEM2-ES
5	CanESM2	17	inmcm4
6	CCSM4	18	IPSL-CM5A-LR
7	CESM1-BGC	19	MIROC-ESM
8	CMCC-CMS	20	MIROC5
9	CNRM-CM5	21	MPI-ESM-LR
10	CSIRO-Mk3-6-0	22	MPI-ESM-MR
11	FGOALS-s2	23	MRI-CGCM3
12	FGOALS-g2	24	NorESM1-M

The five models best able to simulate ENSO teleconnections to Australian precipitation are given as bold text

Southern Slopes (SS), the Southern and South-Western Flatlands (SSWF), and the Wet Tropics (WT). These clusters are depicted in Fig. 1. See CSIRO and Bureau of Meteorology (2015) for further details.

2.5 Model assessment

As noted by Power and Delage (2018), while the ability of climate models to simulate ENSO has improved (Flato et al. 2013), the simulation of ENSO in the latest generation of climate models is not perfect (Flato et al. 2013; Power et al. 2013; Bellenger et al. 2018). Additionally some models fail to capture the teleconnection between the tropical Pacific and Australia, including ENSO rainfall teleconnections (King et al. 2015). While imperfect, the models do exhibit skill in simulating the sign of the difference between spatially averaged El Niño and La Niña precipitation (“E–L”)

in the overwhelming majority of locations around the world examined by Power and Delage (2018), including Northern Australia and Southern Australia/New Zealand.

We investigated this further here, finding that the multi-model mean sign of spatially averaged E–L is the same as the observed sign in all eight NRM clusters using June–November precipitation.

In Figs. 6 and 7 (described in detail later) we stratify results according to ENSO phases. In the corresponding analysis we restrict attention to the five models that best simulate ENSO precipitation teleconnections to Australia. To identify these models, we evaluated the models using two additional metrics. The first assesses the pattern of the ENSO teleconnection map for Australian precipitation over the whole country, while the second assesses the magnitude of ENSO-driven variability in all of the NRM clusters individually.

The first metric is equal to the spatial correlation coefficient between the observed and simulated teleconnections map for each model. The teleconnection maps are based on the correlation map between Australia June–November precipitation in year t and the November (year t)–April (year $t + 1$) Niño3.4 SST. The spatial correlation coefficients are generally low. For example, 13 models had spatial correlation coefficients < 0.2 . These models were excluded. With the second metric we examined the magnitude of E–L in each NRM cluster. Six of the models that could not simulate the magnitude of E–L within a range of $\pm 50\%$ in four or more NRM clusters were excluded. Only five models were retained through this process: ACCESS1.3, CMCC-CMS, CESM1-BGC, GFDL-ESM2M, and NorESM1-M. The spatial correlation coefficients for these models ranged from 0.35 to 0.5 and they simulated the magnitude of E–L in 4–6 of the eight NRM clusters.

2.6 Decile thresholds and definition of drought

In this study we examine changes in Winter–Spring (June–November) Decile thresholds and the frequency with which precipitation falls below the Decile 1 threshold. Note that there are nine such thresholds separating ten Deciles. We use the term “drought” for cases when precipitation over the Winter–Spring season falls below the lowest decile (Decile 1) threshold under pre-industrial conditions. This is similar to the definition used by the Australian Bureau of Meteorology, which defines “drought” as rainfall over a three-month period being in the lowest decile of what has been recorded since 1900.

3 Results

Projected multi-model mean changes between the historical period and the 21st Century under the RCP8.5 scenario, using all 24 models, are depicted in Fig. 2. The figure shows that the spatial structure of changes in the mean and in decile breaks 1–9 have a similar structure and a similar magnitude in most areas. This is consistent with external forcing driving a shift in the distribution of precipitation over the region to a lower value, with little change in the shape of the distribution. We will examine contrasts between the various panels, the corresponding shape changes, and their implications later.

Note again, that all of the results in this paper refer to Winter–Spring rainfall.

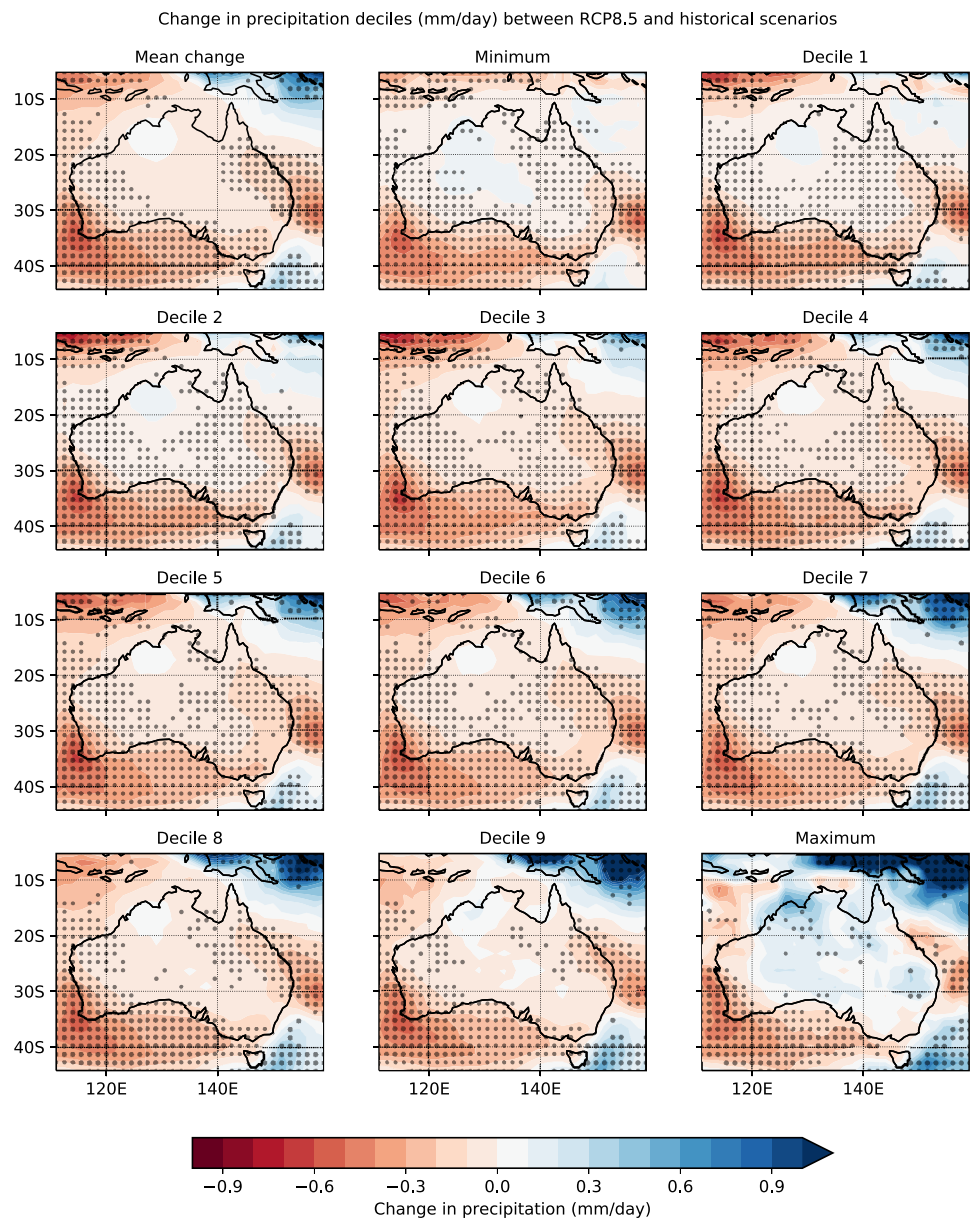
3.1 Changes linked to Decile 1

The value of the Decile 1 threshold declines over most of the country (Fig. 2, right hand upper panel), apart from the northwest, where there is little change. This panel is similar to Fig. 3, which shows the change in the percentage of years that are below the pre-industrial Decile 1 value, from the twentieth century to the twenty-first century. Values vary from a decrease of a few percent in the northwest, to increases of more 10% in most of southern Australia, with increases over 30% in the southwest and about 15–20% in Victoria. Approximately 60% of years are projected to fall below the preindustrial Decile 1 value near Perth in southwest WA, about 35% near Adelaide in South Australia, 30% of years near Melbourne, 19% of years near Sydney, 23% of years in Canberra, and about 25% of years near Brisbane.

3.2 Changes in the frequency of droughts occurring in consecutive Winter–Spring seasons

Here we examine droughts when consecutive Winter–Spring seasons all fall below the lowest decile (Decile 1) under preindustrial conditions. Consecutive years of low precipitation during the Winter–Spring season can be damaging to ecosystems and impact management of water, bushfires and agricultural systems. The number of “droughts” of length 1–6 consecutive years is depicted in Fig. 4 for the historical period and for the twenty-first century under the RCP8.5 scenario. Each NRM cluster is considered separately. The plots indicate that the multi-model median number of droughts of duration 1–4 years tends to increase in all of the NRM clusters in the twenty-first century relative to the twentieth century. During the twentieth century, 3-year droughts occur very infrequently. In fact, among the 24 simulations examined, two simulations at most produce three-year droughts in

Fig. 2 Projected changes in the mean, Deciles 1–9 thresholds, the minimum and the maximum between RCP8.5 (2010–2099) and the historical simulations (1900–1989). Stippling indicates that more than 70% of models agree on the sign of the change. All panels represent multi-model mean changes. June–November (mm/day)



the NRM clusters. Four-year droughts are even less frequent, occurring in one simulation only or not at all in each NRM cluster.

In the twenty-first century under RCP8.5 the frequency of multi-model median one-year droughts increases in every cluster by between 1 and 5 events per century on average. While 5- and 6-year droughts do not occur during the twentieth century, they occur, albeit very infrequently, in the twenty-first century in all clusters. In all clusters there are 1–2 5- and six-year events, except in Southern and Southwestern Flatlands, where the frequency is higher on average.

The increase in the frequency of droughts occurring in consecutive Winter–Spring seasons is clearly an important component of the increase in the frequency of years in drought (i.e., regardless of duration) depicted in Fig. 3.

3.3 Changes in other deciles

If all of the maps in Fig. 2 were identical then this would suggest that external forcing causes precipitation (relative frequency) distributions for all regions to shift, with the shape of the distributions unchanged. However, the maps are not identical, indicating that in some regions external forcing may have also driven a change in the shape of the precipitation distribution. This effect is most clearly seen over the Solomon Islands and PNG near the northern and eastern edges of the plot. Here there is very little change in Decile 1 precipitation, whereas the changes in Deciles 6–9 are large. In this region Deciles 6–9 are higher in the twenty-first century than in the historical and pre-industrial periods.

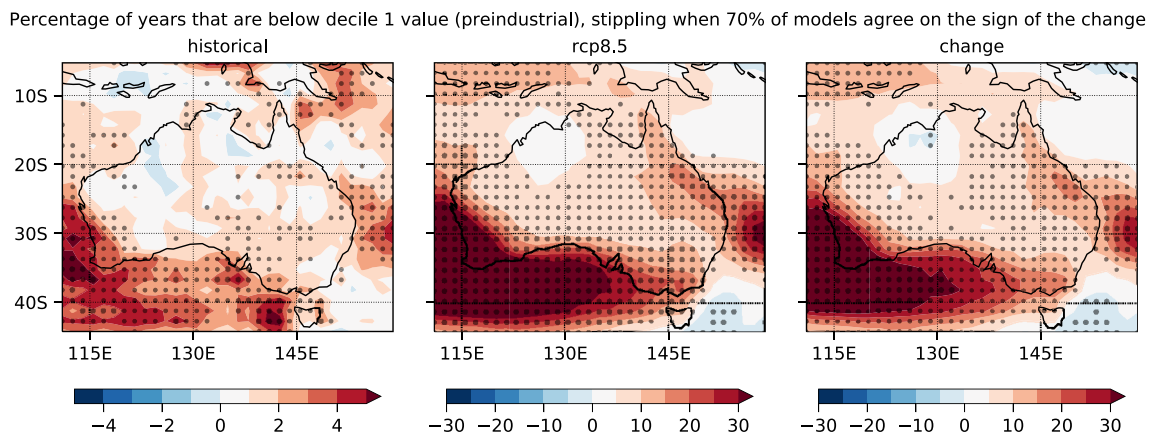


Fig. 3 Percentage of years that precipitation is below the pre-industrial Decile 1 threshold. Historical (twentieth century; left), RCP8.5 (twenty-first century; middle), and the difference between them (i.e.,

RCP8.5–Historical simulation; right). Stippling indicates that more than 70% of models agree on the sign of the change. Multi-model mean changes (%)

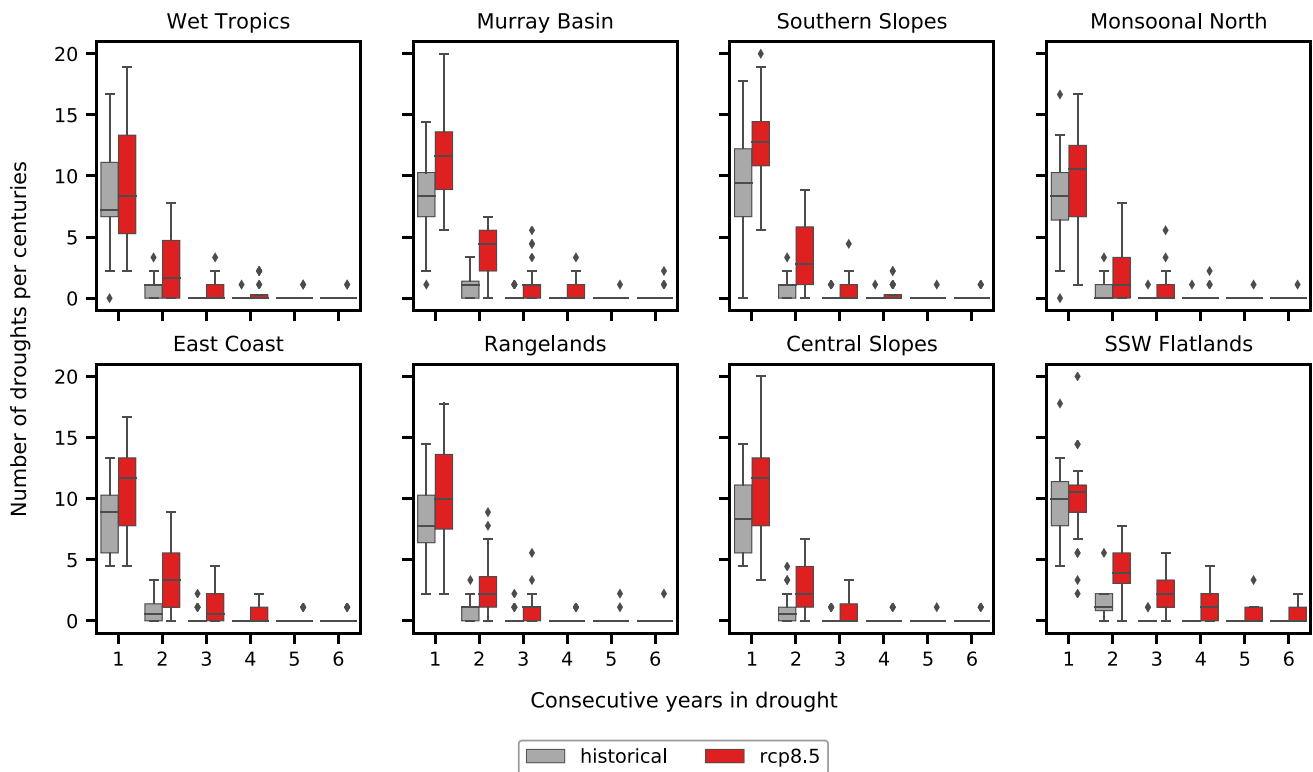


Fig. 4 The number of droughts per century with the duration indicated on X-axis, during the twentieth century (from Historical runs; grey) and the twenty-first century under RCP8.5 (red) for the eight NRM regions. In each case the box shows the interquartile range, the

horizontal lines the median. The whiskers show the rest of the distribution except for outliers—indicated using small black diamonds—that are outside the range $1.5*[Q1, Q3]$, where $[Q1, Q3]$ is the interquartile range

Some of the differences between panels in Fig. 2 are presented in Fig. 5. The top left panel, in conjunction with Fig. 2, shows that the projected reduction in Decile 1 over much of the country is not as great as the projected reduction in Decile 5. There are also differences between the projected change in Decile 1 and Decile 9 precipitation (Fig. 5, bottom

left). For example, Decile 9 increases markedly over PNG and the Solomon Islands whereas Decile 1 does not change much at all in the same region and the magnitude of the reduction in Decile 1 over Victoria and parts of southern NSW tends to be greater than the magnitude of the projected reduction in Decile 9 precipitation.

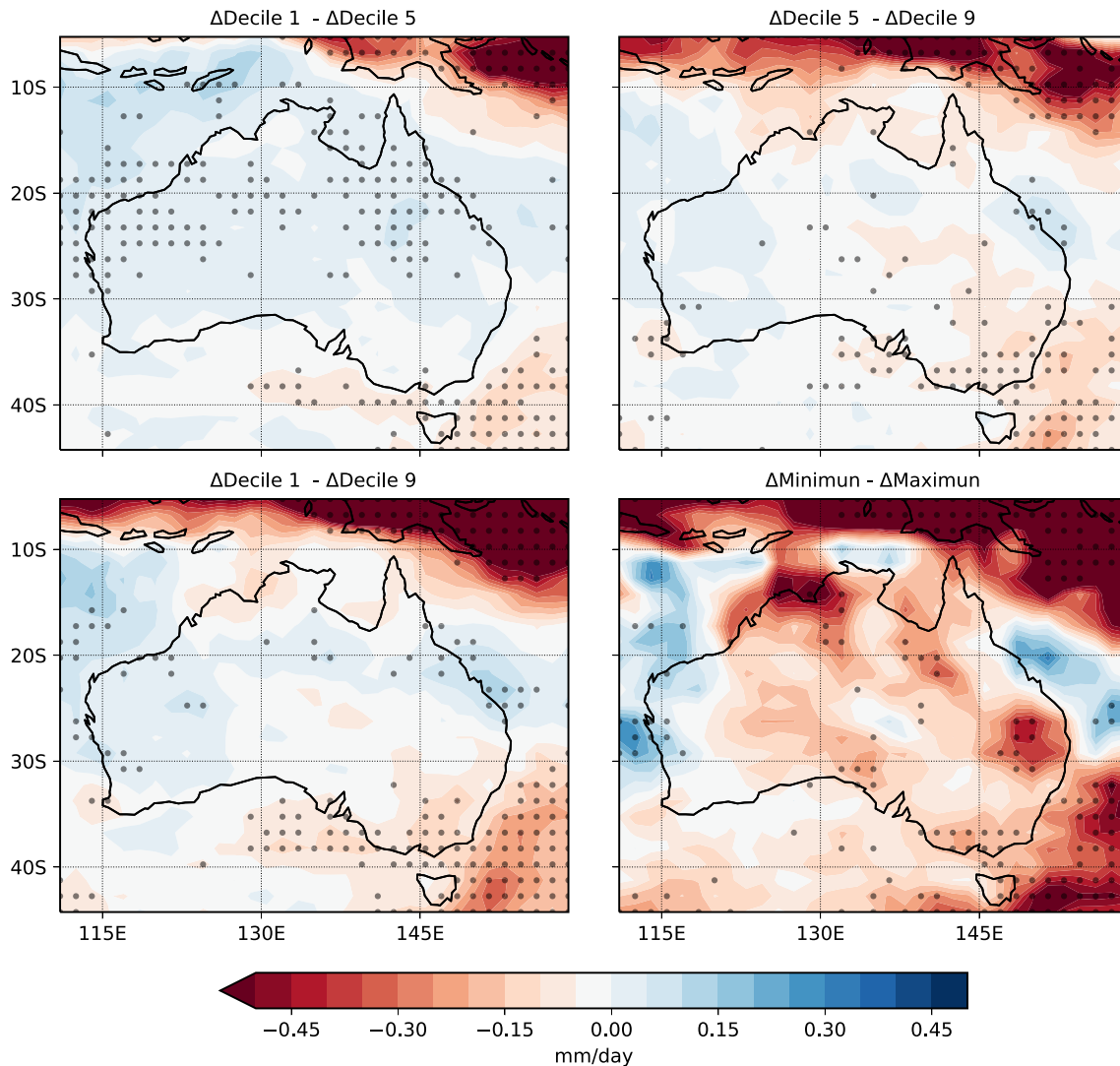


Fig. 5 Differences between some of the panels in Fig. 2: Δ Decile 1– Δ Decile 5 (top left), Δ Decile 5– Δ Decile 9 (top right), Δ Decile 1– Δ Decile 9 (bottom left) and Δ Minimum– Δ Maximum (bottom

right). The changes, e.g., Δ Decile 1, are calculated by subtracting the twentieth century value from the twenty-first century value under RCP8.5. Multi-model mean changes (mm/day)

Asymmetries are also present in the projected changes for minima and maxima (Fig. 5, bottom right). This is also evident in Fig. 2, which shows that changes in the minima are similar to changes in most deciles, whereas maxima do not change much over most of the country, and actually increase in many locations. For example, over north-west Australia the minimum drops while the maximum monthly precipitation value increases, while over Victoria and part of eastern Australia the minimum declines, while the maximum value is unchanged.

In summary, in some locations external forcing, in addition to shifting precipitation distributions, also drives changes in the shape of the precipitation distribution. We will return to this issue below.

3.4 Combined impact of ENSO and external forcing

As noted in the model assessment section, we focus here on the five models that are best able to simulate ENSO teleconnections to Australian rainfall.

The proportion of El Niño years, La Niña years and neutral years resulting in Decile 1 precipitation in the five models with the most realistic ENSO teleconnections is depicted in Fig. 6 during the twentieth century (left column) and the twenty-first century (middle column). The difference between them (i.e., RCP8.5–historical) is also presented (right column).

During the historical period over eastern Australia approximately 15–30% of El Niño years result in Decile

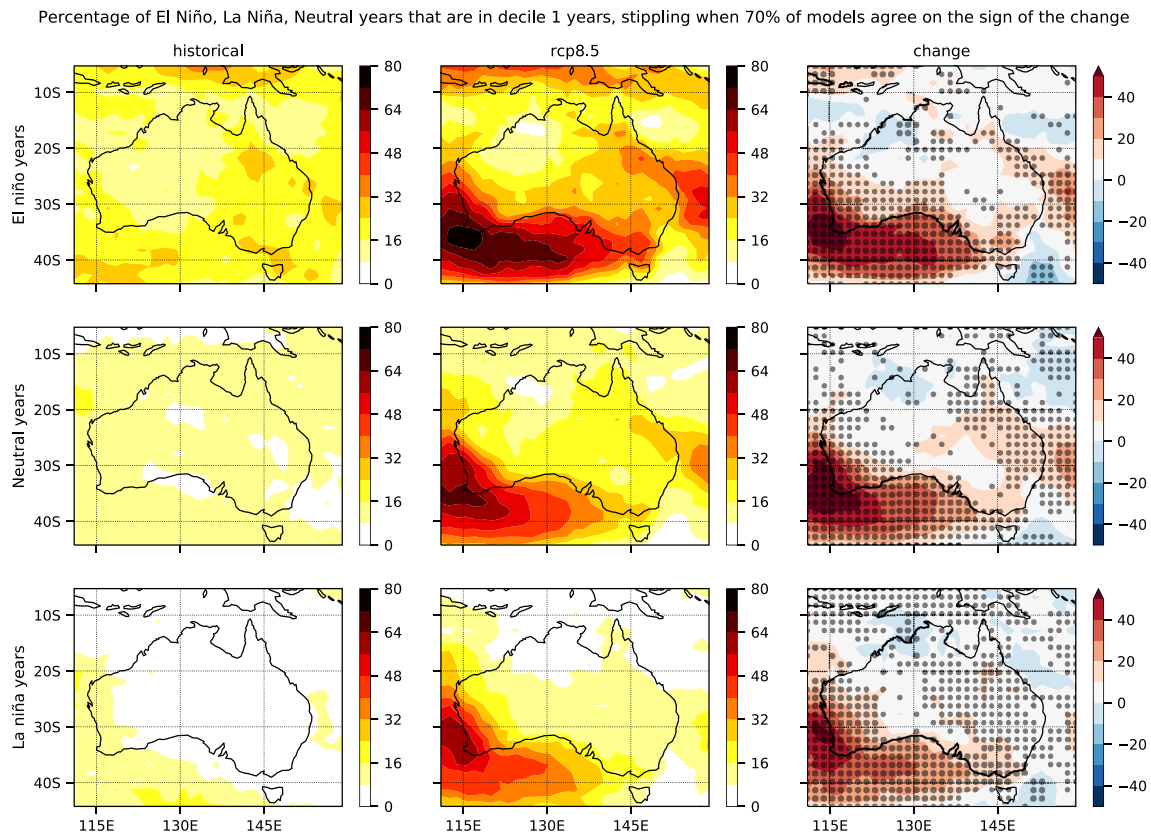


Fig. 6 The percentage of El Niño, La Niña, and neutral years that are in Decile 1. Historical conditions (left column), under RCP8.5 (central column) and the difference RCP8.5–Historical (right column). Multi-model means of five models with most realistic ENSO teleconnections (%)

1 precipitation, whereas only around 4% of La Niña years do. These figures are much larger during the twenty-first century: approximately 25–40% of El Niño years result in Decile 1 precipitation, while approximately 12% of La Niña years do.

In southwest WA approximately 20% of El Niño years and 12% of La Niña years result in Decile 1 precipitation during the twentieth century, whereas during the twenty-first century these figures increase to 70% and over respectively.

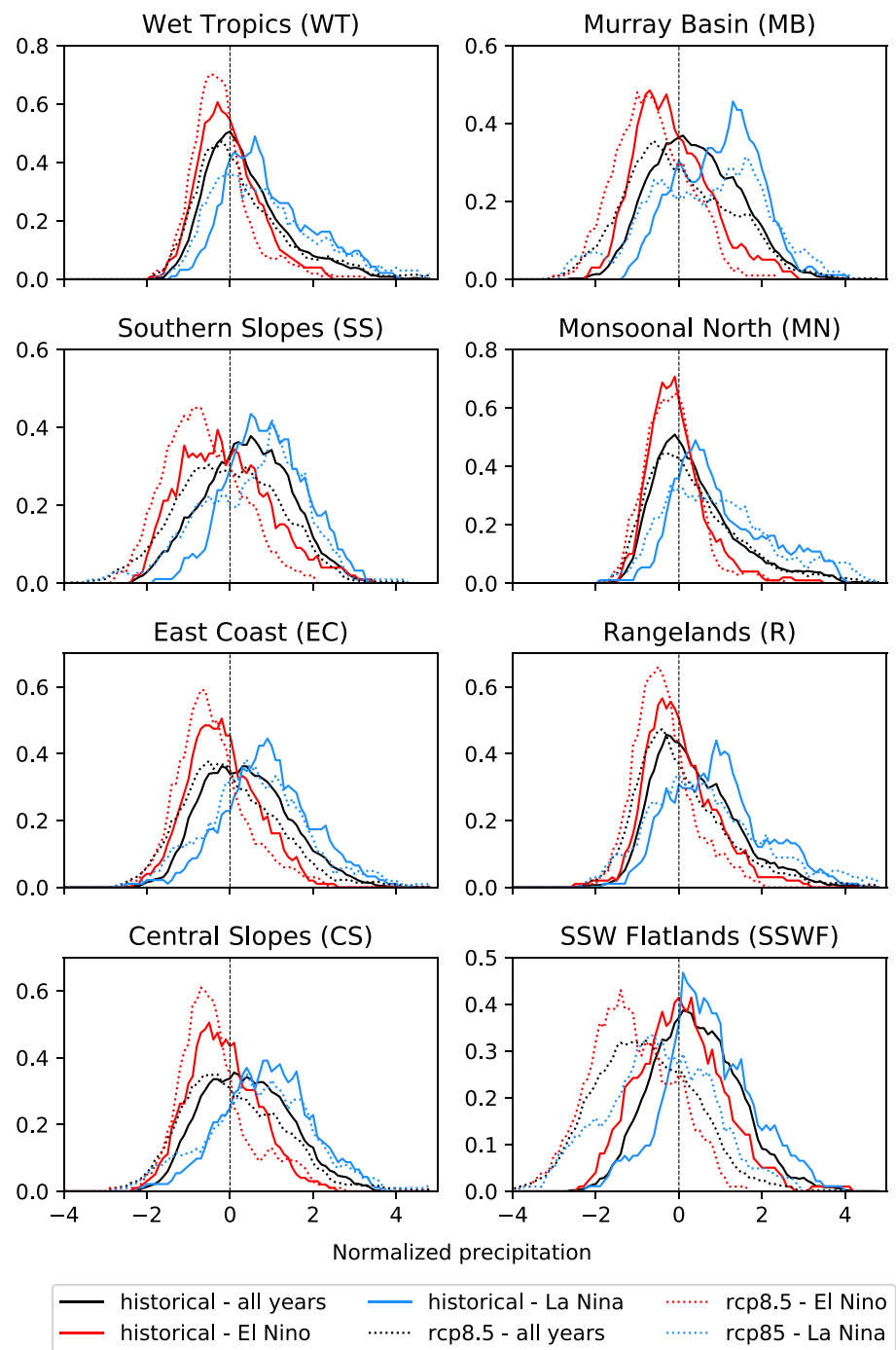
The combined impact of ENSO and climate change on precipitation in the eight NRM clusters is depicted in Fig. 7, which shows standardized precipitation (see caption) distributions for El Niño, La Niña and all years, for the twentieth and twenty-first centuries. The plot indicates that ENSO influences all eight clusters, that El Niño years tend to be drier than La Niña years, and climate change does not change this situation. However, both El Niño and La Niña events tend to be drier during the twenty-first century than they were in the twentieth century. This is as expected from the previous discussion: the twenty-first century distributions for all years, El Niño, and La Niña tend to shift to lower values relative to their twentieth century counterparts. However, we saw above that the results could not be fully explained in terms of shifts alone. The same is true in

seven of the eight panels in Fig. 7 (excluding the Southern and South-western Flatlands): the extreme right-hand (wettest) part of the distributions tend to be little changed or less changed than are the extreme left (driest) parts of the distributions. In fact, in these seven clusters the distributions for La Niña years actually extend further to the right during the twenty-first century than their twentieth century counterparts, albeit marginally. This is consistent with the contrast in the changes in minima and maxima described above (Figs. 2, 5).

3.5 Changes in ENSO variability

We examined changes in ENSO-driven variability—measured using E–L, the difference between El Niño and La Niña precipitation composites—in the eight NRM clusters (Fig. 1) from 1940–1989 to 2050–2099. We found that a while a majority of the five models best able to simulate ENSO teleconnections showed an increase in |E–L| in all clusters, the majority was very marginal in all clusters except the Wet Tropics (4 out of 5 models showing an increase), the Monsoonal North (4 out of 5), the Central Slopes (4 out of 5) and Southern and Southwestern Flatlands (4 out of 5). Increases in precipitation during La Niña years are projected to occur

Fig. 7 Relative frequency distributions of standardized precipitation anomalies in the eight NRM regions. Distributions are provided for all years, El Niño years, and La Niña years in the twentieth and twenty-first centuries. Each model had its historical mean subtracted and the resulting data was scaled by the model's historical standard deviation. Multi-model means of the five models with the most realistic ENSO teleconnections are presented. X-axis units: dimensionless



in the Wet Tropics and Monsoonal North (4 out of 5), while decreases in precipitation during La Niña years are projected for the Southern Slopes (4 out of 5) and Southern and Southwestern Flatlands (5 out of 5). Precipitation during El Niño years is projected to decrease in the Wet Tropics (4 out of 5), the Murray Basin (5 out of 5), the Southern Slopes (5 out of 5), the East Coast (4 out of 5), the Rangelands (4 out of 5) and Southern and Southwestern Flatlands (5 out of 5).

We also examined changes in precipitation variability between the twentieth and twenty-first centuries. This

includes, but is not restricted to, variability driven by ENSO. The results were very marginal. While the multi-model mean variability increased in six of the eight clusters, there is a lot of model-to-model differences and not all models exhibit an increase. The most robust increases occurred in the Southern Slopes where all five models that are best able to simulate ENSO teleconnections project an increase, while four out of the same five models project an increase in the Southern and Southwestern Flatlands.

4 Summary and discussion

We analysed 24 CMIP5 climate models to examine externally-forced changes in the frequency of “droughts”, when June–November precipitation falls below the pre-industrial Decile 1 threshold. The number of droughts increases in the twenty-first century under the RCP8.5 scenario in all eight Natural Resource Management (NRM) clusters. Approximately 60% of years are projected to fall below the pre-industrial Decile 1 value near Perth in southwest WA, about 35% near Adelaide, 30% of years near Melbourne, 19% of years near Sydney, 23% of years in Canberra, and about 25% of years near Brisbane. We also show that the increase in drought frequency is partially due to an increase in the frequency of droughts occurring in consecutive Winter–Spring seasons in all NRM clusters. We find, for example, that five- and six-consecutive Winter–Spring seasons droughts are evident during the twenty-first century, but not during the twentieth century. These new results starkly illustrate an important consequence of the projected decline in mean Winter–Spring rainfall over Southern Australia noted previously (CSIRO-BoM 2011; Power and Delage 2018).

The relative frequency distributions of precipitation shift to lower values in all NRM clusters. However, apart from Southern and Southwestern Flatlands, the shifts are accompanied by changes in the shape of the distributions whereby the high end of the distributions do not shift as much as other parts of the distribution, and extremely wet values are marginally more frequent in the twenty-first century than they are in the twentieth century. This means that in most locations generally drier conditions are projected to be infrequently punctuated by seasons that are just as wet or even wetter than the wettest years experienced during the twentieth century.

While beyond the scope of this study, these projected changes have important implications for ecosystems, and the management of water, bushfires and agricultural systems. In fact water managers have already implemented changes in response to projections and the drier conditions that are already occurring in southern Australasia (Power et al. 2005; Reisinger et al. 2015).

While the multi-model mean sign of the difference between El Niño and La Niña precipitation composites matches the sign of the observed difference in all eight NRM clusters, the models generally do a poor job in simulating ENSO precipitation teleconnections over Australia. In the models best able to reproduce the teleconnections there is a marked increase in the proportion of El Niño and La Niña years resulting in Decile 1 precipitation over eastern Australian under RCP8.5.

An increase in ENSO-driven variability is suggested for the Wet Tropics, the Monsoonal North, the Central Slopes

and Southern and Southwestern Flatlands under the same scenario. There is also a suggestion of an increase in inter-annual variability in the Southern Slopes and the Southern and Southwestern Flatlands. However, given the limited number of models that exhibit skill in simulating ENSO teleconnections, and consequently the limited number of models upon which these results are based, these results should be regarded as hypotheses for further testing using CMIP6 models, which will hopefully simulate ENSO teleconnections more accurately.

Acknowledgements This work is supported by the Earth System and Climate Change Hub of the Australian National Environmental Science Program. We acknowledge the World Climate Research Programme’s Working Group on Coupled Modelling, which is responsible for CMIP, and we thank the climate modelling groups for producing and making available their model output. For CMIP the U.S. Department of Energy’s Program for Climate Model Diagnosis and Intercomparison provides coordinating support and led development of software infrastructure in partnership with the Global Organization for Earth System Science Portals. Many of the figures were produced using Python. We also thank two anonymous reviewers for constructive comments.

Open Access This article is licensed under a Creative Commons Attribution 4.0 International License, which permits use, sharing, adaptation, distribution and reproduction in any medium or format, as long as you give appropriate credit to the original author(s) and the source, provide a link to the Creative Commons licence, and indicate if changes were made. The images or other third party material in this article are included in the article’s Creative Commons licence, unless indicated otherwise in a credit line to the material. If material is not included in the article’s Creative Commons licence and your intended use is not permitted by statutory regulation or exceeds the permitted use, you will need to obtain permission directly from the copyright holder. To view a copy of this licence, visit <http://creativecommons.org/licenses/by/4.0/>.

References

- Bellenger H, Guilyardi E, Leloup J et al (2018) ENSO representation in climate models : from CMIP3 to CMIP 1999–2018 <https://doi.org/10.1007/s00382-013-1783-z>
- CSIRO, Bureau of Meteorology (2015) Climate change in Australia: Technical Report
- Flato G, Marotzke J, Abiodun B, et al (2013) Evaluation of climate models 9. In: Climate change 2013: the physical science basis. Contribution of working group I to the fifth assessment report of the intergovernmental panel on climate change
- King AD, Donat MG, Alexander LV, Karoly DJ (2015) The ENSO–Australian rainfall teleconnection in reanalysis and CMIP5. *Clim Dyn*. <https://doi.org/10.1007/s00382-014-2159-8>
- Morice CP, Kennedy JJ, Rayner NA, Jones PD (2012) Quantifying uncertainties in global and regional temperature change using an ensemble of observational estimates: The HadCRUT4 data set. *J Geophys Res Atmos* 117:1–22. <https://doi.org/10.1029/2011JD017187>
- Moss RH, Edmonds JA, Hibbard KA et al (2010) The next generation of scenarios for climate change research and assessment. *Nature* 463:747–756

- Power S, Delage F, Chung C et al (2013) Robust twenty-first-century projections of El Niño and related precipitation variability. *Nature* 502:541–545. <https://doi.org/10.1038/nature12580>
- Power SB, Delage FPD (2018) El Niño-Southern oscillation and associated climatic conditions around the world during the latter half of the twenty-first century. *J Clim*. <https://doi.org/10.1175/JCLI-D-18-0138.1>
- Power SB, Sadler B, Nicholls N (2005) The influence of climate science on water management in Western Australia: Lessons for climate scientists. *Bull Am Meteorol Soc*. <https://doi.org/10.1175/BAMS-86-6-839>
- Raupach MR, Briggs PR, Haverd V et al (2009) Australian water availability project. CSIRO Marine and Atmospheric Research, Component: Final Report for Phase 3
- Reisinger A, Kitching RL, Chiew F et al (2015) Australasia. In: *Climate change 2014: impacts, adaptation and vulnerability: Part B: regional aspects: working group II contribution to the fifth assessment report of the intergovernmental panel on climate change*
- Taylor KE, Stouffer RJ, Meehl GA (2007) A summary of the CMIP5. *Exp Des* 4:1–33
- van Vuuren DP, Edmonds J, Kainuma M et al (2011) The representative concentration pathways: an overview. *Clim Change* 109:5–31. <https://doi.org/10.1007/s10584-011-0148-z>

Publisher's Note Springer Nature remains neutral with regard to jurisdictional claims in published maps and institutional affiliations.